Eur J Nucl Med Mol Imaging (2010) 37:613–622
DOI 10.1007/s00259-009-1283-x

ORIGINAL ARTICLE

# Imaging of EGFR expression in murine xenografts using site-specifically labelled anti-EGFR $^{111}$In-DOTA-$Z_{EGFR:2377}$ Affibody molecule: aspect of the injected tracer amount

**Vladimir Tolmachev · Daniel Rosik · Helena Wållberg · Anna Sjöberg · Mattias Sandström · Monika Hansson · Anders Wennborg · Anna Orlova**

Received: 4 June 2009 / Accepted: 13 September 2009 / Published online: 17 October 2009


**Abstract**
*Introduction* Overexpression of epidermal growth factor receptor (EGFR) is a prognostic and predictive biomarker in a number of malignant tumours. Radionuclide molecular imaging of EGFR expression in cancer could influence patient management. However, EGFR expression in normal tissues might complicate in vivo imaging. The aim of this study was to evaluate if optimization of the injected protein dose might improve imaging of EGFR expression in tumours using a novel EGFR-targeting protein, the DOTA-$Z_{EGFR:2377}$ Affibody molecule.
*Methods* An anti-EGFR Affibody molecule, $Z_{EGFR:2377}$, was labelled with $^{111}$In via the DOTA chelator site-specifically conjugated to a C-terminal cysteine. The affinity of DOTA-$Z_{EGFR:2377}$ for murine and human EGFR was measured by surface plasmon resonance. The cellular processing of $^{111}$In-DOTA-$Z_{EGFR:2377}$ was evaluated in vitro. The biodistribution of radiolabelled Affibody molecules injected in a broad range of injected Affibody protein doses was evaluated in mice bearing EGFR-expressing A431 xenografts.
*Results* Site-specific coupling of DOTA provided a uniform conjugate possessing equal affinity for human and murine EGFR. The internalization of $^{111}$In-DOTA-$Z_{EGFR:2377}$ by A431 cells was slow. In vivo, the conjugate accumulated specifically in xenografts and in EGFR-expressing tissues. The curve representing the dependence of tumour uptake on the injected Affibody protein dose was bell-shaped. The highest specific radioactivity (lowest injected protein dose) provided a suboptimal tumour-to-blood ratio. The results of the biodistribution study were confirmed by γ-camera imaging.
*Conclusion* The $^{111}$In-DOTA-$Z_{EGFR:2377}$ Affibody molecule is a promising tracer for radionuclide molecular imaging of EGFR expression in malignant tumours. Careful optimization of protein dose is required for high-contrast imaging of EGFR expression in vivo.

**Keywords** Affibody molecules · EGFR · Indium-111 · Gamma-camera imaging

V. Tolmachev (✉) · A. Orlova
Unit of Biomedical Radiation Sciences, Rudbeck Laboratory, Uppsala University,
751 81 Uppsala, Sweden
e-mail: vladimir.tolmachev@bms.uu.se

D. Rosik · A. Sjöberg · M. Hansson · A. Wennborg
Affibody AB,
Bromma, Sweden

H. Wållberg
School of Biotechnology, Royal Institute of Technology,
Stockholm, Sweden

M. Sandström
Department of Medical Physics, Uppsala University Hospital,
Uppsala, Sweden

V. Tolmachev
Department of Medical Sciences, Nuclear Medicine, Uppsala University,
Uppsala, Sweden

## Introduction

Epidermal growth factor receptor (EGFR; other designations HER1 and erbB-1) is a transmembrane tyrosine kinase

receptor involved in the regulation of cell proliferation, apoptosis, and motility [1]. EGFR is often overexpressed in different kinds of malignant tumours and clinical data show that overexpression of EGFR can be used as a prognostic biomarker in, for example, lung [2], colorectal [3], breast [4], prostate [5] and ovarian [6] carcinomas, and soft-tissue sarcomas [7]. High levels of EGFR expression in tumours can predict local-regional relapse after radiotherapy of head and neck squamous cell carcinomas [8] and can help select patients who will benefit from hyperfractionated accelerated radiotherapy [9]. High EGFR expression is also a predictive biomarker for a poor response to preoperative radiotherapy in advanced rectal carcinoma [10] and for tamoxifen treatment of early-stage breast cancer [11]. However, the common method of determination of EGFR levels, biopsy with subsequent immunohistochemistry, is associated with problems, such as expression heterogeneity, discordance of EGFR expression in primary tumours and metastases [12], inadequate procedures and antibodies [6, 7] and alteration of EGFR status during therapy [13]. The use of radionuclide molecular imaging might overcome many of these problems [14], and considerable effort has been invested in the development of EGFR imaging probes (for the latest reviews see references [15, 16]).

The use of targeting proteins and peptides is a promising way to create EGFR imaging probes. Both radiolabelled anti-EGFR monoclonal antibodies (Mabs) [17–23] and the natural ligand, epidermal growth factor (EGF) [19–29], have been evaluated for this purpose. Although both preclinical and clinical studies using radiolabelled intact antibodies have demonstrated their capacity to image EGFR-expressing tumours, the sensitivity of intact antibody-based tracers is limited by their long blood residence time and slow tumour accumulation, which reduces target to nontarget contrast. For example, direct head-to-head comparison of EGF (6 kDa) and the anti-EGFR Mab 528 (about 150 kDa) has demonstrated that the smaller EGF provides superior image contrast [19]. The observed mismatch between the EGFR expression level in xenografts and the uptake of the radiolabelled Mab cetuximab [21, 23] might be a reflection of problems with vascular permeability of Mabs or with elevated nonspecific tumour uptake of macromolecules, or a combination of both. The use of radiolabelled EGF also has its limitations. Adverse reactions (nausea, vomiting, diarrhoea, hypotension, fever and chills) were recorded when the amount of injected EGF was escalated to find the optimal protein dose for imaging using $^{131}$I-EGF [24]. Due to these physiological reactions, it would be of great interest to develop an imaging probe which is as small as EGF, but does not possess agonistic action.

A possible way to develop small targeting proteins is to use a variant of molecular display to isolate Affibody molecules binding to specific targets. Affibody molecules are small (6–7 kDa) proteins based on the 58 amino acid scaffold (Z domain) structurally derived from staphylococcal protein A [30]. Randomization of 13 surface-exposed amino acids in their three-helix structure has provided a library from which high-affinity binde rs to different targets have been selected [31, 32]. The feasibility of developing Affibody molecules that are suitable as radionuclide imaging probes for visualization of EGFR-expressing xenografts in vivo has been demonstrated using dimeric $^{111}$In-CHX-A″-DTPA-$(Z_{EGFR:955})_2$ (apparent dissociation constant ($K_D$) approximately 1 n*M*) [33]. The anti-EGFR Affibody molecule $Z_{EGFR:1907}$, with a monomeric affinity in the low nanomolar range, was obtained by affinity maturation [34]. With this tracer, residualizing radiometal labels provide better contrast in in vivo imaging than nonresidualizing halogens [35]. It has also been shown that the monomeric form of the $Z_{EGFR:1907}$ Affibody molecule is a better imaging probe than the dimeric variant, presumably due to better extravasation and tissue penetration [35].

Further affinity maturation of the first generation of anti-EGFR Affibody molecules was performed to provide subnanomolar affinity. A single cysteine was introduced at the C-terminus to enable site-specific labelling [36–38]. A maleimido derivative of the versatile DOTA chelator was coupled to this cysteine, providing a well-defined homogeneous conjugate suitable for labelling with a number of radiometals. The next step, in vivo evaluation, required serious consideration due to the expression of EGFR in normal organs and tissues. Previous experiments with $^{111}$In-labelled EGF showed specific, saturable uptake in murine liver, spleen, stomach, pancreas, intestines, and submaxillary salivary gland due to the expression of EGFR in these organs [39]. Further studies in murine xenograft models demonstrated that the amount of injected $^{68}$Ga-DOTA-EGF influences tumour-to-organ ratios due to the saturation of uptake in normal organs with low levels of EGFR expression [29]. The models were adequate in these studies since there is cross-reactivity between human EGF and murine EGFR and vice versa. The relevance of the animal model is determined by the cross-reactivity of anti-human EGFR tracers with EGFR in the model animal. Therefore, an anti-EGFR Affibody molecule $Z_{EGFR:2377}$, which binds with equal affinity to human and murine EGFR, was selected for the current study.

The goal of this study was to determine in a murine xenograft model if optimization of the injected $Z_{EGFR:2377}$ Affibody protein dose (i.e. the specific activity) might improve the tumour-to-organ contrast in radionuclide imaging of EGFR expression.

## Materials and methods

### Materials and instrumentation

Maleimido-mono-amide-DOTA (1,4,7,10-tetraazacyclododecane-1,4,7-tris-acetic acid-10-maleimidoethylacetamide) was purchased from Macrocyclics (Dallas, TX). $^{111}$In-indium chloride was purchased from Covidien (Hazelwood, MO). The EGFR-rich squamous carcinoma cell line A431 was obtained from American Type Culture Collection (ATCC, Rockville, MD). Silica gel-impregnated glass fibre sheets for instant thin-layer chromatography (ITLC SG) were from Gelman Sciences (Ann Arbor, MI). The distribution of radioactivity along the ITLC strips was measured on a Cyclone storage phosphor system and analysed using OptiQuant image analysis software (both from PerkinElmer). The radioactivity in samples was measured using an automated gamma-counter with a 3-inch NaI(Tl) detector (1480 WIZARD, Wallac Oy, Turku, Finland). Statistical analysis of data on cellular uptake and biodistribution was performed using GraphPad Prism (version 4.00 for Windows; GraphPad Software, San Diego, CA) in order to determine significant differences ($p<0.05$).

### Preparation and characterization of DOTA-conjugated Affibody molecules

The selection of $Z_{EGFR:2377}$ will be reported elsewhere. For site-specific coupling of the chelator, a C–terminal cysteine was introduced into $Z_{EGFR:2377}$ according to methods described previously [36]. Recombinant production and purification of the cysteine-containing Affibody molecule was performed as described by Ahlgren et al. [37]. Before conjugation, a solution of Affibody molecules was treated with dithiothreitol (DTT; E. Merck, Darmstadt, Germany) in order to reduce spontaneously formed intermolecular disulphide bonds. For this purpose, a stock solution of Affibody molecules (2 ml, 2.3 mg/ml in PBS) was mixed with 100 µl 1 *M* Tris-HCl buffer, pH 8.0, and 63 µl DTT solution (0.5 *M* in water). The mixture was incubated at 40°C for 30 min. The reduced Affibody molecules were then purified and the buffer was changed according to the manufacturer's instructions using a disposable PD-10 column (GE Healthcare) pre-equilibrated with 0.2 *M* sodium acetate, pH 5.5. Maleimido-mono-amide-DOTA (2 mg) was added and the mixture incubated for 1 h at 40°C.

The Affibody molecules were purified and analysed by high-performance liquid chromatography and on-line mass spectrometry (HPLC-MS) using an Agilent 1100 LC/MSD system equipped with electrospray ionization and single quadrupole (Agilent Technologies, Palo Alto, CA). For purification, a Zorbax 300SB C18 9.4×250 5 µm column was used. The analysis was performed using a Zorbax 300SB-C18, 2.1×150 mm 3.5 µm column. Solvent A comprised 0.1% trifluoroacetic acid (TFA) in water, and solvent B comprised 0.1% TFA in acetonitrile. The column oven temperature was set to 30°C. For analysis, the column was eluted with a linear gradient of 10% to 70% solvent B over 15 min, with a flow rate of 0.5 ml/min. The purified conjugate (further designated as DOTA-$Z_{EGFR:2377}$) was freeze-dried. Chemstation Rev. B.02.01 software (Agilent) was used for analysis and evaluation of HPLC data.

The affinity of the Affibody molecule for both human and mouse EGFR was analysed using a Biacore 2000 instrument. Briefly, human EGFR and mouse EGFR-Fc (both from R&D Systems) were immobilized in different flow cells of a CM5 chip using amine coupling according to the manufacturer's instructions. The immobilization level for both target proteins was 780 resonance units (RU). DOTA-$Z_{EGFR:2377}$ was diluted to 1,000, 250, 62, 16 and 4 n*M* in HBS-EP buffer (10 mmol/l HEPES, 150 mmol/l NaCl, 3 mmol/l EDTA, 0.005% surfactant P-20, pH 7.4) and injected over the immobilized proteins using HBS-EP as running buffer and a flow rate of 50 µl/min. The apparent dissociation equilibrium constant ($K_D$) was calculated using BIAevaluation 3.2 software, using a binding model for parallel reactions. To ensure that labelling conditions would not decrease the binding capacity of DOTA-$Z_{EGFR:2377}$ to EGFR, the conjugate was dissolved in 0.2 *M* ammonium acetate, pH 5.5, and was incubated at 60°C for 30 min. Sensograms of treated conjugate and nontreated control were recorded for both human EGFR and mouse EGFR-Fc at 400 n*M* concentration of DOTA-$Z_{EGFR:2377}$ in HBS-EP buffer.

For labelling, DOTA-$Z_{EGFR:2377}$ was reconstituted in 0.2 *M* ammonium acetate buffer, pH 5.5, to a concentration of 1 mg/ml. For a typical labelling 30 µl of DOTA-$Z_{EGFR:2377}$ solution was mixed with 100 µl 0.2 *M* ammonium acetate buffer, pH 5.5, and 15 MBq $^{111}$In. The reaction mixture was incubated at 60°C for 30 min and the radiochemical purity was evaluated using ITLC eluted with 0. 2 *M* citric acid.

The in vitro binding specificity of $^{111}$In-DOTA-$Z_{EGFR:2377}$ was verified using EGFR-expressing A431 cervical carcinoma cells by receptor presaturation with unlabelled Affibody molecules as described by Wållberg and Orlova [40]. Cellular retention and internalization of radioactivity was evaluated using A431 cells as described by Wållberg and Orlova [40].

### In vivo studies

The animal experiments were planned and performed in accordance with national regulations on laboratory animal protection and were approved by the local Ethics Committee for Animal Research in Uppsala. Female outbred

BALB/c nu/nu mice were used in all experiments. Xenografts of the EGFR-expressing A431 squamous carcinoma cell line were established by subcutaneous injection of $10^7$ cells implanted in the hind leg, and the tumours were grown for 10–14 days before the experiment. At the time of the study, the average tumour weight was 0.2±0.1 g. The animals were randomized into groups of four.

To evaluate the influence of injected Affibody protein dose (i.e. specific activity in the case of constant injected activity) on the targeting properties, a series of $^{111}$In-DOTA-$Z_{EGFR:2377}$ formulations with various predetermined specific radioactivity was prepared. An aliquot of $^{111}$In-DOTA-$Z_{EGFR:2377}$ was diluted with a stock solution of nonlabelled DOTA-$Z_{EGFR:2377}$ in PBS to provide injection doses containing 0.1 μg (0.013 nmol), 5 μg (0.63 nmol), 30 μg (3.8 nmol), 50 μg (6.3 nmol), 100 μg (12.5 nmol) and 150 μg (18.6 nmol) DOTA-$Z_{EGFR:2377}$ labelled with 30 kBq $^{111}$In (17.5 fmol) per mouse. The preparations were diluted with PBS to provide an injection volume of 100 μL per mouse. The preparations were injected intravenously into tumour-bearing mice, and 4 h after injection, the animals were injected intraperitoneally with a lethal dose of anaesthetic solution and killed by heart puncture. The blood was withdrawn into a heparinized syringe and collected. Salivary glands, liver, kidneys, tumour and samples of muscle were excised from the animals. In addition, the gastrointestinal tract with its content and the carcass were collected. The radioactivity of the samples was measured and the uptake in tumours and healthy tissues was calculated as percent of injected radioactivity per gram (% IA/g), except for the gastrointestinal tract and carcass, for which the data were expressed as %IA per sample. One group of four mice was killed and dissected 24 h after injection of 50 μg conjugate.

A gamma-camera imaging experiment was performed to obtain a visual confirmation of the results obtained in the ex-vivo measurements. Two mice were injected intravenously with 100 μL PBS solution containing 5 μg of DOTA-$Z_{EGFR:2377}$ (7.5 MBq $^{111}$In-DOTA-$Z_{EGFR:2377}$). Another two animals were injected with a solution containing 50 μg of DOTA-$Z_{EGFR:2377}$ (7.5 MBq $^{111}$In-DOTA-$Z_{EGFR:2377}$). The animals were injected with a lethal dose of Ketalar-Rompun solution 4 h after injection and killed by cervical dislocation. In order to remove any radioactivity interfering with the imaging, the urinary bladders were excised. The animals were simultaneously imaged using a Millennium VG (General Electric) gamma camera equipped with a medium energy general purpose (MEGP) collimator. The scintigraphic results were evaluated visually and analysed quantitatively using Hermes software (Nuclear Diagnostics). Quantitative analysis was performed by drawing equal regions of interest over the tumour and the contralateral thigh. Tumour-to-nontumour ratios were calculated on the basis of average count per pixel in each region of interest.

## Results

### Preparation and characterization of DOTA-conjugated Affibody molecules

The described coupling and purification procedure provided >99% pure DOTA-$Z_{EGFR:2377}$ conjugate (molecular weight: calculated 7916.9 Da, found by MS 7914.13 Da; the difference is within accuracy of the method).

The Biacore sensograms (Fig. 1) for binding of DOTA-$Z_{EGFR:2377}$ to human and mouse EGFR were similar. The best curve fitting was found using a parallel reactions model. The apparent dissociation constants were found to be nearly the same, with the difference within the accuracy of the method. Values of $K_{D1}$ were 0.9 and 0.8 n*M* for human and mouse EGF, respectively. Corresponding values of $K_{D2}$ were 28 and 28 n*M*. Additional experiments showed that the labelling conditions (incubation in 0.2 *M* ammonium acetate, pH 5.5, at 60°C for 30 min) did not influence binding of DOTA-$Z_{EGFR:2377}$ to either human or mouse EGFR (data not shown).

For labelling of DOTA-$Z_{EGFR:2377}$ with a specific radioactivity of 0.5 MBq/μg (3.96 GBq/μmol), the radiochemical purity of $^{111}$In-DOTA-$Z_{EGFR:2377}$ was 98±2%. This enabled the use of $^{111}$In-DOTA-$Z_{EGFR:2377}$ for biological studies without additional purification.

In the in vitro specificity test, presaturation of EGFR receptors in A431 cells with nonlabelled Affibody molecules reduced the cell-bound radioactivity from 17.6±0.3% to 1.3±0.1% ($p<10^{-6}$) after 1 h incubation with $^{111}$In-DOTA-$Z_{EGFR:2377}$ at 37°C. This demonstrated that binding of $^{111}$In- DOTA-$Z_{EGFR:2377}$ to EGFR-expressing cells was specific. The cellular retention and internalization test of $^{111}$In-DOTA-$Z_{EGFR:2377}$ showed that the conjugate was efficiently retained by EGFR-expressing cells (Fig. 2). The cellular retention of the total radioactivity was good, with 53.6±0.2% cell-associated radioactivity after 24 h incubation at 37°C. The main radioconjugate release occured within the first 0.5 h with a slow increase in released radioactivity up to 4 h. Thereafter, the levels were almost stable up to 24 h. The internalization of $^{111}$In-DOTA-$Z_{EGFR:2377}$ was relatively slow, with less than 15% internalized radioactivity after 24 h.

### Biodistribution study

The biodistribution of radioactivity 4 h after injection of different specific activities of $^{111}$In-DOTA-$Z_{EGFR:2377}$ into BALB/C nu/nu mice bearing EGFR-expressing A431

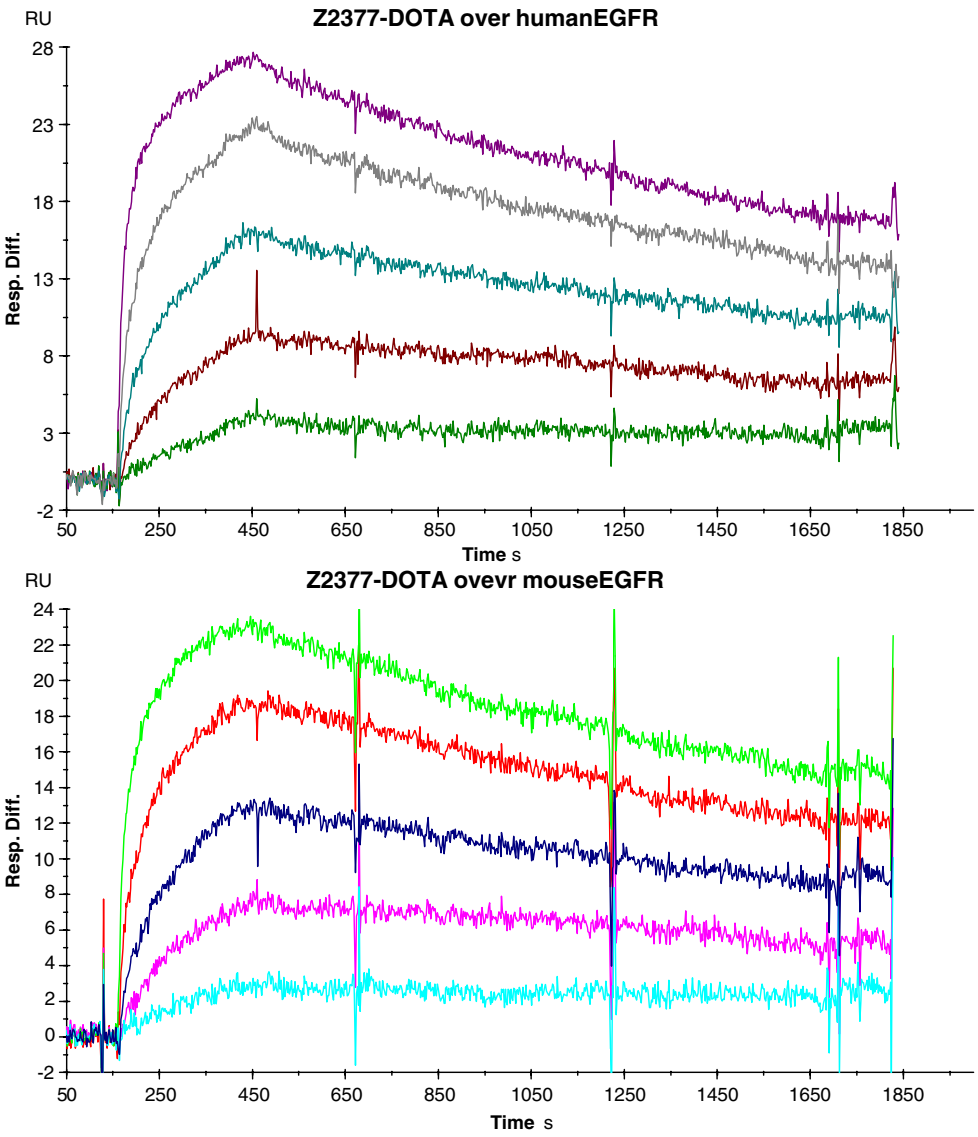


**Fig. 1** Sensograms obtained after injection of the DOTA-$Z_{EGFR:2377}$ over a flow-cell surface with immobilized human EGFR (*upper panel*) or mouse EGFR-Fc (*lower panel*) at concentrations of 1,000, 250, 62, 16 and 4 n*M*

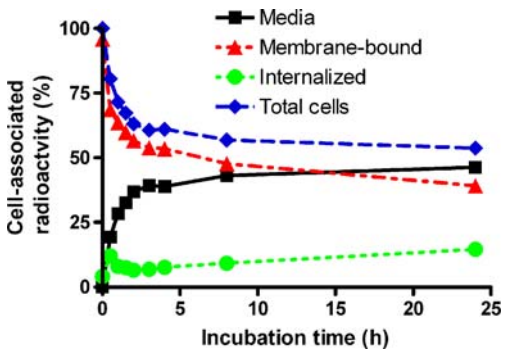


**Fig. 2** Cell-associated radioactivity as a function of time after interrupted incubation of A431 cells with $^{111}$In-DOTA-$Z_{EGFR:2377}$. The cell associated radioactivity at time zero after the interrupted incubation was considered 100%. The radioactivity that was removed from cells by treatment with 4 *M* urea solution in 0.2 *M* glycine buffer, pH 2.0, was considered membrane-bound, and the rest internalized. Data are presented as means±SD ($n$=3); error bars are not visible as they are smaller than the point symbols

xenografts is shown in Fig. 3. The uptake of radioactivity in the liver after injection of 0.1 or 5 μg DOTA-$Z_{EGFR:2377}$ was approximately equal. Increasing the injected Affibody protein dose to 30 μg decreased the uptake of radioactivity in the liver. However, increasing the injected protein dose beyond 50 μg did not decrease the liver uptake further. A similar effect was observed in salivary glands, another organ with high EGFR expression, although the effect on uptake of increasing the injected amount was more pronounced. The blood level of radioactivity decreased with increasing injected protein dose. The kidney level was approximately constant. The dependence of tumour uptake on the injected dose was bell-shaped, with a maximum between 30 and 50 μg injected protein. The same pattern was found for accumulation of radioactivity in the gastrointestinal tract and retention in the carcass. The influence of injected protein dose on radioactivity uptake

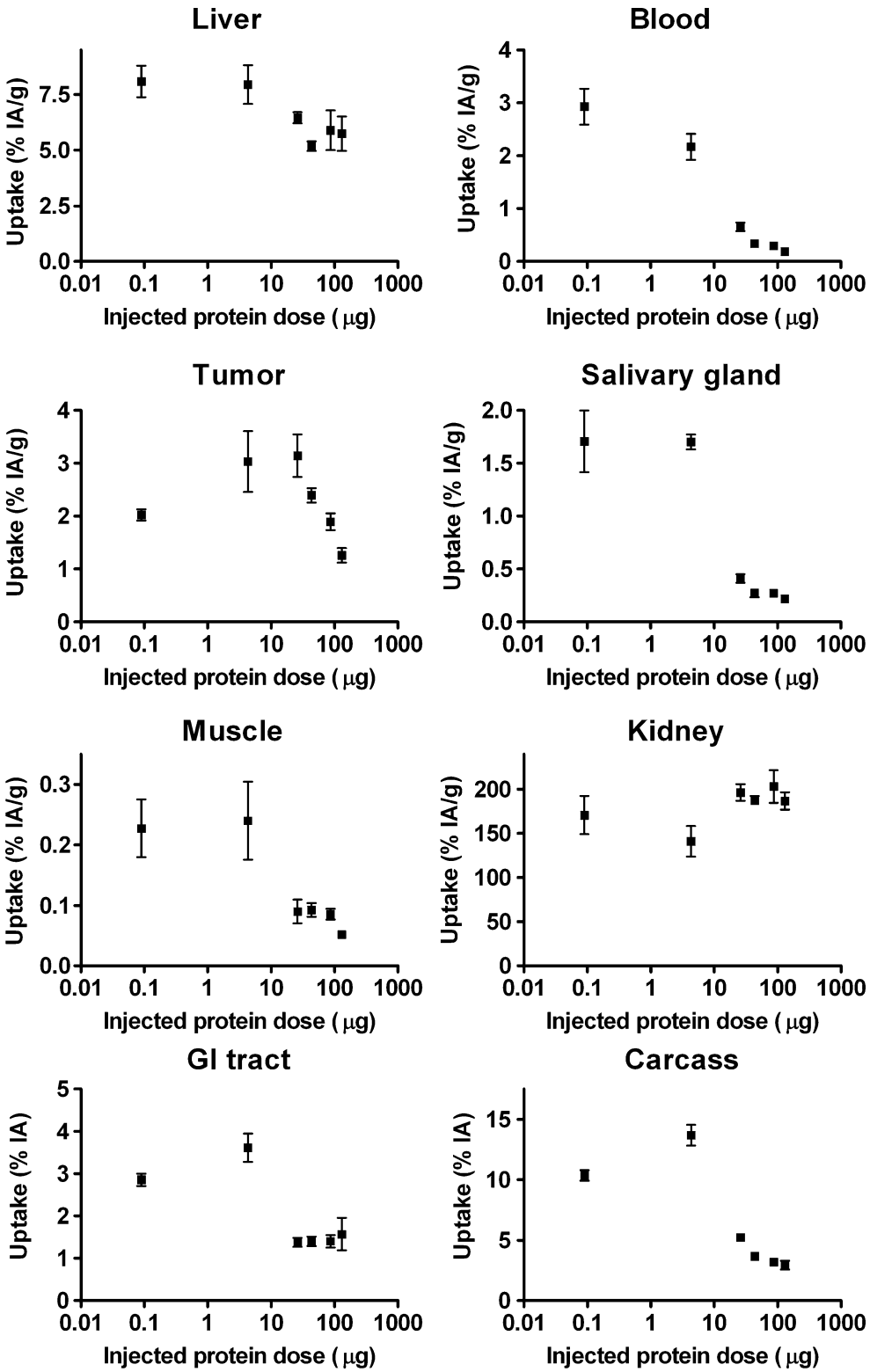


**Fig. 3** Uptake of radioactivity 4 h after injection of 0.1–150 μg $^{111}$In-DOTA-$Z_{EGFR:2377}$ in six groups of mice (for each group $n$=4). Data are presented as average %IA/g and SD. The data for the gastrointestinal tract (with contents) and carcass are presented as %IA per whole sample

was translated into an effect on tumour-to-organ ratios (Fig. 4). Tumour-to-organ ratios reached either a maximum or a plateau at 50 μg of injected protein.

Comparing the biodistribution profiles at 4 and 24 h after injection of 50 μg (the optimal injected dose) of $^{111}$In-labelled DOTA-$Z_{EGFR:2377}$ (Table 1) demonstrated constant uptake levels of radioactivity in the liver and salivary glands (no statistically significant difference between 4 and 24 h after injection). The radioactivity levels in other organs and tissues, as well as in tumour, decreased over time.

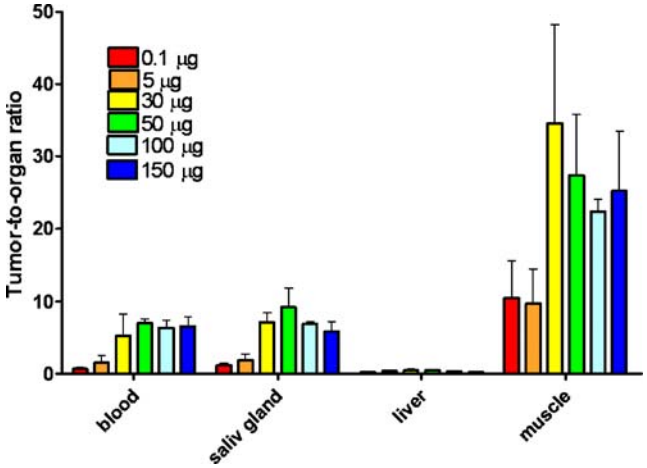


**Fig. 4** Tumour-to-organ ratios 4 h after injection of 0.1–150 μg $^{111}$In-DOTA-$Z_{EGFR:2377}$ in six groups of mice (for each group $n$=4). Data are presented as average and SD

However, the clearance from tumour was slower than from normal organs and tissues which improved the tumour-to-blood ratio at the later time point (Table 2).

γ-Camera imaging 4 h after injection confirmed the results of the biodistribution experiments. The most prominent site of radioactivity accumulation for both protein doses of $^{111}$In-DOTA-$Z_{EGFR:2377}$ was the kidneys. The EGFR-expressing xenografts were visualized using both doses. However, the use of 50 μg of $^{111}$In-DOTA-$Z_{EGFR:2377}$ provided considerably better image contrast. The tumour-to-contralateral side ratios were 5.0±0.3 and 2.2±0.0 for 50 μg and 5 μg injected $^{111}$In-DOTA-$Z_{EGFR:2377}$, respectively.

## Discussion

The results of this study demonstrate that the new anti-EGFR $Z_{EGFR:2377}$ Affibody molecule can be site-specifically conjugated with maleimido-derivative of DOTA by introduction of a single cysteine into the cysteine-free Affibody scaffold. Coupling with such a versatile chelator as DOTA allows stable labelling of peptides with a variety of nuclides, such as $^{111}$In for SPECT [37], and $^{68}$Ga [41], $^{86}$Y [42] and $^{55}$Co [43] for PET. In vitro studies using both cell culture and surface plasmon resonance showed that the conjugate retained specificity and affinity for EGFR. Importantly, the conjugate can be purified to homogeneity providing a tracer with well-defined targeting and biodistribution properties. Equal affinity of DOTA-$Z_{EGFR:2377}$ for murine and human EGFR is another important feature of the conjugate, rendering mice with human xenografts a relevant model for assessment of biodistribution in humans.

In vivo biodistribution studies demonstrated specificity of $^{111}$In-DOTA-$Z_{EGFR:2377}$ in targeting in vivo both human and murine EGFR, since an increase in the injected protein dose of the conjugate led to a significant decrease in uptake in A431 xenografts and EGFR-expressing organs (liver and salivary gland; Fig. 3), most likely due to receptor saturation. An interesting feature of the biodistribution profile was the decrease in blood radioactivity concentration with increased the protein dose. The same phenomenon has also been observed with the a previous generation of anti-EGFR Affibody molecules [35]. We have previously hypothesized that this might be due to dissociation of Affibody molecules from EGFR-expressing organs, but we could not prove this since the standard in vitro internalization assay (acid wash), showing internalization at 4°C, does not work with Affibody molecules. In the present study a new internalization assay was used based on the combination of low pH and high molar strength of a urea solution for removal of membrane-bound Affibody molecules. This assay confirmed that internalization of $^{111}$In-DOTA-$Z_{EGFR:2377}$ is relatively slow (Fig. 2). Thus, membrane-bound $^{111}$In-DOTA-$Z_{EGFR:2377}$ might dissociate from EGFR and re-enter the blood circulation. Therefore, we suggest that EGFR-expressing tissues may act as a depot for $^{111}$In-DOTA-$Z_{EGFR:2377}$ slowly releasing membrane-

**Table 1** Biodistribution of $^{111}$In-DOTA-$Z_{EGFR:2377}$ 4 h and 24 h after injection of 50 μg into BALB/C nu/nu mice bearing A431 xenografts. Data are presented as average %IA/g ±SD ($n$=4), except for the gastrointestinal tract and carcass which are presented as %IA per sample

| | 4h after injection | 24h after injection |
|---|---|---|
| Blood | 0.34±0.02 | 0.12±0.03* |
| Salivary glands | 0.27±0.08 | 0.18±0.10 |
| Liver | 5.12±0.4 | 5.1±0.5 |
| Kidneys | 187±9 | 144±20* |
| Tumour | 2.4±0.3 | 1.6±0.2* |
| Muscle | 0.09±0.02 | 0.06±0.03 |
| Gastrointestinal tract | 1.4±0.2 | 0.7±0.2* |
| Carcass | 3.6±0.4 | 2.3±0.2* |

*$p$<0.05, uptake at 4 h vs. 24 h after injection (unpaired $t$ test).

**Table 2** Tumour-to-organ ratios of $^{111}$In-DOTA-$Z_{EGFR:2377}$ 4 h and 24 h after injection of 50 μg into BALB/C nu/nu mice bearing A431 xenografts. Data are average of four animals ±SD

| | 4h after injection | 24h after injection |
|---|---|---|
| Blood | 7.0±0.5 | 14.3±3.6* |
| Salivary gland | 9.2±2.5 | 11.3±5.6 |
| Liver | 0.46±0.02 | 0.32±0.05* |
| Kidney | 0.000±0.000 | 0.01±0.00 |
| Muscle | 27±8 | 34±18 |

*$p$<0.05, 4 h vs. 24 h after injection.

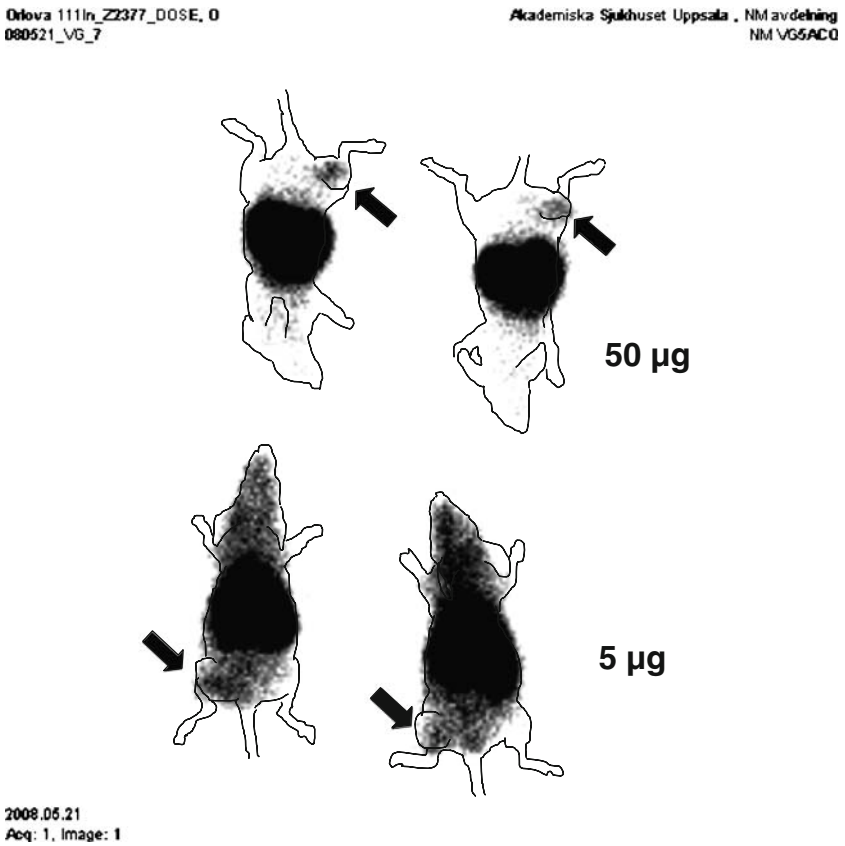


**Fig. 5** Planar γ-camera images of EGFR expression in A431 xenografts in BALB/c nude mice using $^{111}$In-DOTA-$Z_{EGFR:2377}$. The images were obtained simultaneously 4 h after administration of 5 or 50 μg of the tracer (*arrows* tumour)

bound tracer. Indeed, increasing the dose of nonlabelled DOTA-$Z_{EGFR:2377}$ reduced the blood-born radioactivity presumably by the saturation of available binding sites in EGFR-expressing healthy tissues. As expected, this would also lead to a reduction in the radioactivity level in tissues which do not express EGFR, but are in equilibrium with the blood (e.g. muscle). For tumours, the dependence of uptake on the injected Affibody protein dose displays a bell-shaped curve (Fig. 3). The initial increase in uptake was apparently associated with saturation of EGFR in organs with low natural expression, which resulted in more $^{111}$In-DOTA-$Z_{EGFR:2377}$ available for tumour targeting. However, a further increase in the injected dose resulted in progressive saturation of EGFR in tumours and decreased radioactivity accumulation. Tumour-to-organ ratios, which determine image contrast, also demonstrated a maximum or plateau around 50 μg per animal (Fig. 4). γ-Camera imaging demonstrated that the use of the optimal injected $^{111}$In-DOTA-$Z_{EGFR:2377}$ dose improved the contrast of EGFR imaging in comparison with the use of lower dose (higher specific radioactivity) of the conjugate (Fig. 5).

The results of this study are in good agreement with clinical data. For example, Divgi et al. [18] reported that elevated doses of $^{111}$In-labelled anti-EGFR Mab 225 (at least 20 mg, preferably 120 mg) were required for imaging of EGFR-expressing squamous cell carcinoma of the lung, while lower doses resulted in radioactivity accumulation predominantly in the hepatic compartment. The data also indicated a decrease in tumour uptake when the Mab dose exceeded 120 mg. Dose dependence was not found in studies of radiolabelled cetuximab (chimeric variant of 225) in rodents [20–23]. However, it should be noted that cetuximab does not interact with hepatic tissue in rodents [44]. Most likely the rodent model is not adequate for studying this aspect of targeting of EGFR if the difference in the tracer affinity for human and murine receptor is large. With cetuximab, the tumour-to-blood ratio did not exceed 5 for A431 xenografts in mice even several days after injection. Despite the added complexity of affinity for the murine EGFR in the liver, the present tracer is superior, displaying a tumour-to-blood ratio of 7 at 4 h after injection and twice this value at 24 h after injection, disregarding some differences in the experimental procedures used. Recently, imaging of EGFR in a murine xenograft model, using an engineered antibody fragment called Nanobody, has been reported [45]. This small (15 kDa) tracer provides an appreciably better tumour-to-blood ratio in the murine model than the ratio expected for intact Mabs. However, no data for cross-reactivity with murine EGFR were presented, making it difficult to compare its imaging properties with those of $^{111}$In-DOTA-$Z_{EGFR:2377}$.

High specific radioactivity of a radiolabelled imaging peptide or protein is often considered as a requirement for

successful imaging. This is true when target expression is low or a potent agonistic action of the imaging probe puts restrictions on the injectable mass from a safety perspective. On the other hand, expression of a molecular target in healthy organs or the presence of shed target in the circulation may require an increased dose of the targeting agent. A bell-shaped dependence of tumour-to-organ ratios has been described for other targeting peptides, such as somatostatin [46] and bombesin [47] analogues. Our study shows that optimization of the injected dose of an imaging probe is also necessary for imaging of EGFR. The use of artificial ligands, such as Affibody molecules, is an advantage in this case because they can be selected as pharmacologically neutral or even antagonistic, and a physiological action would therefore not restrict the optimization.

## Conclusion

This study demonstrated that the new generation of monomeric Affibody molecules, site-specifically labelled using DOTA, are suitable for radionuclide imaging of EGFR overexpression in malignant tumours. A careful optimization of the dose of injected imaging probe is required for improvement of contrast, and hence, sensitivity of EGFR imaging.

**Acknowledgments** This study was supported by grants from the Swedish Cancer Society (Cancerfonden) and the Swedish Research Council (Vetenskapsrådet). We thank Veronika Eriksson and the staff of the animal facility at Rudbeck Laboratory for technical assistance.

**Disclosures** The authors, Orlova Anna, Helena Wållberg and Vladimir Tolmachev had earlier, and Daniel Rosik, Anna Sjöberg, Monika Hansson, Anders Wennborg have currently an affiliation (employment) with Affibody AB, Bromma, Sweden, which holds the intellectual property rights and trademarks for Affibody molecules.

## References

1. Yarden Y. The EGFR family and its ligands in human cancer. Signalling mechanisms and therapeutic opportunities. Eur J Cancer. 2001;37(Suppl 4):S3–8.
2. Selvaggi G, Novello S, Torri V, Leonardo E, De Giuli P, Borasio P, et al. Epidermal growth factor receptor overexpression correlates with a poor prognosis in completely resected non-small-cell lung cancer. Ann Oncol. 2004;15:28–32.
3. Zlobec I, Vuong T, Hayashi S, Haegert D, Tornillo L, Terracciano L, et al. A simple and reproducible scoring system for EGFR in colorectal cancer: application to prognosis and prediction of response to preoperative brachytherapy. Br J Cancer. 2007;96:793–800.
4. Nieto Y, Nawaz F, Jones RB, Shpall EJ, Nawaz S. Prognostic significance of overexpression and phosphorylation of epidermal growth factor receptor (EGFR) and the presence of truncated EGFRvIII in locoregionally advanced breast cancer. J Clin Oncol. 2007;25:4405–13.
5. Schlomm T, Kirstein P, Iwers L, Daniel B, Steuber T, Walz J, et al. Clinical significance of epidermal growth factor receptor protein overexpression and gene copy number gains in prostate cancer. Clin Cancer Res. 2007;13:6579–84.
6. Psyrri A, Kassar M, Yu Z, Bamias A, Weinberger PM, Markakis S, et al. Effect of epidermal growth factor receptor expression level on survival in patients with epithelial ovarian cancer. Clin Cancer Res. 2005;11:8637–43.
7. Kersting C, Packeisen J, Leidinger B, Brandt B, von Wasielewski R, Winkelmann W, et al. Pitfalls in immunohistochemical assessment of EGFR expression in soft tissue sarcomas. J Clin Pathol. 2006;59:585–90.
8. Ang KK, Berkey BA, Tu X, Zhang HZ, Katz R, Hammond EH, et al. Impact of epidermal growth factor receptor expression on survival and pattern of relapse in patients with advanced head and neck carcinoma. Cancer Res. 2002;62:7350–6.
9. Bentzen SM, Atasoy BM, Daley FM, Dische S, Richman PI, Saunders MI, et al. Epidermal growth factor receptor expression in pretreatment biopsies from head and neck squamous cell carcinoma as a predictive factor for a benefit from accelerated radiation therapy in a randomized controlled trial. J Clin Oncol. 2005;23:5560–7.
10. Giralt J, de las Heras M, Cerezo L, Eraso A, Hermosilla E, Velez D, et al. The expression of epidermal growth factor receptor results in a worse prognosis for patients with rectal cancer treated with preoperative radiotherapy: a multicenter, retrospective analysis. Radiother Oncol. 2005;74:101–8.
11. Giltnane JM, Rydén L, Cregger M, Bendahl PO, Jirström K, Rimm DL. Quantitative measurement of epidermal growth factor receptor is a negative predictive factor for tamoxifen response in hormone receptor positive premenopausal breast cancer. J Clin Oncol. 2007;25:3007–14.
12. Scartozzi M, Bearzi I, Berardi R, Mandolesi A, Fabris G, Cascinu S. Epidermal growth factor receptor (EGFR) status in primary colorectal tumors does not correlate with EGFR expression in related metastatic sites: implications for treatment with EGFR-targeted monoclonal antibodies. J Clin Oncol. 2004;22:4772–8.
13. Choong LY, Lim S, Loh MC, Man X, Chen Y, Toy W, et al. Progressive loss of epidermal growth factor receptor in a subpopulation of breast cancers: implications in target-directed therapeutics. Mol Cancer Ther. 2007;6:2828–42.
14. Pantaleo MA, Nannini M, Maleddu A, Fanti S, Nanni C, Boschi S, et al. Experimental results and related clinical implications of PET detection of epidermal growth factor receptor (EGFr) in cancer. Ann Oncol. 2009;20:213–26.
15. Gelovani JG. Molecular imaging of epidermal growth factor receptor expression-activity at the kinase level in tumors with positron emission tomography. Cancer Metastasis Rev. 2008;27:645–53.
16. Mishani E, Abourbeh G, Eiblmaier M, Anderson CJ. Imaging of EGFR and EGFR tyrosine kinase overexpression in tumors by nuclear medicine modalities. Curr Pharm Des. 2008;14:2983–98.
17. Goldenberg A, Masui H, Divgi C, Kamrath H, Pentlow K, Mendelsohn J. Imaging of human tumor xenografts with an indium-111-labeled anti-epidermal growth factor receptor monoclonal antibody. J Natl Cancer Inst. 1989;81:1616–25.
18. Divgi CR, Welt S, Kris M, Real FX, Yeh SD, Gralla R, et al. Phase I and imaging trial of indium 111-labeled anti-epidermal growth factor receptor monoclonal antibody 225 in patients with squamous cell lung carcinoma. J Natl Cancer Inst. 1991;83:97–104.
19. Reilly RM, Kiarash R, Sandhu J, Lee YW, Cameron RG, Hendler A, et al. A comparison of EGF and MAb 528 labeled with 111In for imaging human breast cancer. J Nucl Med. 2000;41:903–11.
20. Cai W, Chen K, He L, Cao Q, Koong A, Chen X. Quantitative PET of EGFR expression in xenograft-bearing mice using 64Cu-

labeled cetuximab, a chimeric anti-EGFR monoclonal antibody. Eur J Nucl Med Mol Imaging. 2007;34:850–8.
21. Milenic DE, Wong KJ, Baidoo KE, Ray GL, Garmestani K, Williams M, et al. Cetuximab: preclinical evaluation of a monoclonal antibody targeting EGFR for radioimmunodiagnostic and radioimmunotherapeutic applications. Cancer Biother Radiopharm. 2008;23:619–31.
22. Ping Li W, Meyer LA, Capretto DA, Sherman CD, Anderson CJ. Receptor-binding, biodistribution, and metabolism studies of 64Cu-DOTA-cetuximab, a PET-imaging agent for epidermal growth-factor receptor-positive tumors. Cancer Biother Radiopharm. 2008;23:158–71.
23. Aerts HJ, Dubois L, Perk L, Vermaelen P, van Dongen GA, Wouters BG, et al. Disparity between in vivo EGFR expression and 89Zr-labeled cetuximab uptake assessed with PET. J Nucl Med. 2009;50:123–31.
24. Cuartero-Plaza A, Martínez-Miralles E, Rosell R, Vadell-Nadal C, Farré M, Real FX. Radiolocalization of squamous lung carcinoma with 131I-labeled epidermal growth factor. Clin Cancer Res. 1996;2:13–20.
25. Rusckowski M, Qu T, Chang F, Hnatowich DJ. Technetium-99m labeled epidermal growth factor-tumor imaging in mice. J Pept Res. 1997;50:393–401.
26. Capala J, Barth RF, Bailey MQ, Fenstermaker RA, Marek MJ, Rhodes BA. Radiolabeling of epidermal growth factor with 99mTc and in vivo localization following intracerebral injection into normal and glioma-bearing rats. Bioconjug Chem. 1997;8:289–95.
27. Sundberg AL, Orlova A, Bruskin A, Gedda L, Carlsson J, Blomquist E, et al. [(111)In]Bz-DTPA-hEGF: preparation and in vitro characterization of a potential anti-glioblastoma targeting agent. Cancer Biother Radiopharm. 2003;18(4):643–54.
28. Babaei MH, Almqvist Y, Orlova A, Shafii M, Kairemo K, Tolmachev V. [99mTc]HYNIC-hEGF, a potential agent for imaging of EGF receptors in vivo: preparation and pre-clinical evaluation. Oncol Rep. 2005;13:1169–75.
29. Velikyan I, Sundberg AL, Lindhe O, Höglund AU, Eriksson O, Werner E, et al. Preparation and evaluation of (68)Ga-DOTA-hEGF for visualization of EGFR expression in malignant tumors. J Nucl Med. 2005;46(11):1881–8.
30. Nygren PA. Alternative binding proteins: affibody binding proteins developed from a small three-helix bundle scaffold. FEBS J. 2008;275:2668–76.
31. Nilsson FY, Tolmachev V. Affibody molecules: new protein domains for molecular imaging and targeted tumor therapy. Curr Opin Drug Discov Devel. 2007;10:167–75.
32. Orlova A, Feldwisch J, Abrahmsén L, Tolmachev V. Update: affibody molecules for molecular imaging and therapy for cancer. Cancer Biother Radiopharm. 2007;22:573–84.
33. Nordberg E, Orlova A, Friedman M, Tolmachev V, Ståhl S, Nilsson FY, et al. In vivo and in vitro uptake of 111In, delivered with the affibody molecule (ZEGFR:955)2, in EGFR expressing tumour cells. Oncol Rep. 2008;19:853–7.
34. Friedman M, Orlova A, Johansson E, Eriksson TL, Höidén-Guthenberg I, Tolmachev V, et al. Directed evolution to low nanomolar affinity of a tumor-targeting epidermal growth factor receptor-binding affibody molecule. J Mol Biol. 2008;376:1388–402.
35. Tolmachev V, Friedman M, Sandström M, Eriksson TL, Rosik D, Hodik M, et al. Affibody molecules for epidermal growth factor receptor targeting in vivo: aspects of dimerization and labeling chemistry. J Nucl Med. 2009;50:274–83.
36. Mume E, Orlova A, Larsson B, Nilsson AS, Nilsson FY, Sjöberg S, et al. Evaluation of ((4-hydroxyphenyl)ethyl)maleimide for site-specific radiobromination of anti-HER2 affibody. Bioconjug Chem. 2005;16:1547–55.
37. Ahlgren S, Orlova A, Rosik D, Sandström M, Sjöberg A, Baastrup B, et al. Evaluation of maleimide derivative of DOTA for site-specific labeling of recombinant affibody molecules. Bioconjug Chem. 2008;19:235–43.
38. Tolmachev V, Xu H, Wållberg H, Ahlgren S, Hjertman M, Sjöberg A, et al. Evaluation of a maleimido derivative of CHX-A" DTPA for site-specific labeling of affibody molecules. Bioconjug Chem. 2008;19:1579–87.
39. Tolmachev V, Orlova A, Wei Q, Bruskin A, Carlsson J, Gedda L. Comparative biodistribution of potential anti-glioblastoma conjugates [111In]DTPA-hEGF and [111In]Bz-DTPA-hEGF in normal mice. Cancer Biother Radiopharm. 2004;19:491–501.
40. Wållberg H, Orlova A. Slow internalization of anti-HER2 synthetic affibody monomer $^{111}$In-DOTA-$Z_{HER2:342}$-pep2: implications for development of labeled tracers. Cancer Biother Radiopharm. 2008;23:435–42.
41. Maecke HR, Hofmann M, Haberkorn U. 68Ga-labeled peptides in tumor imaging. J Nucl Med. 2005;46(Suppl 1):172S–8S.
42. Biddlecombe GB, Rogers BE, de Visser M, Parry JJ, de Jong M, Erion JL, et al. Molecular imaging of gastrin-releasing peptide receptor-positive tumors in mice using 64Cu- and 86Y-DOTA-(Pro1,Tyr4)-bombesin(1-14). Bioconjug Chem. 2007;18:724–30.
43. Wållberg H, Ahlgren S, Widström C, Orlova A. Evaluation of the radiocobalt-labeled [MMA-DOTA-Cys$^{61}$]-$Z_{HER2:2395}$-Cys Affibody molecule for targeting of HER2-expressing tumors. Mol Imaging Biol 2009. doi:10.1007/s11307-009-0238-8.
44. ImClone Systems Incorporated. Cetuximab: epidermal growth factor receptor (EGFR) antibody, version 9.0. ImClone Investigator Brochure. New York: ImClone Systems, 2003.
45. Gainkam LO, Huang L, Caveliers V, Keyaerts M, Hernot S, Vaneycken I, et al. Comparison of the biodistribution and tumor targeting of two 99mTc-labeled anti-EGFR nanobodies in mice, using pinhole SPECT/micro-CT. J Nucl Med. 2008;49:788–95.
46. de Jong M, Breeman WA, Bernard BF, et al. Tumour uptake of the radiolabelled somatostatin analogue [DOTA0,TYR3]octreotide is dependent on the peptide amount. Eur J Nucl Med. 1999;26:693–8.
47. Schuhmacher J, Zhang H, Doll J, Mäcke HR, Matys R, Hauser H, et al. GRP receptor-targeted PET of a rat pancreas carcinoma xenograft in nude mice with a 68Ga-labeled bombesin(6-14) analog. J Nucl Med. 2005;46:691–9.